

Reaction-Diffusion Model for A + A Reaction

Katja Lindenberg*

Department of Chemistry and Institute for Nonlinear Science, University of California, San Diego,
La Jolla, California 92093-0340

Panos Argyrakis† and Raoul Kopelman

Departments of Chemistry and Physics, The University of Michigan, Ann Arbor, Michigan 48109-1055

Received: September 12, 1994; In Final Form: December 28, 1994[⊗]

We formulate an approach to the $A + A \rightarrow$ products reaction that is based on a reaction-diffusion equation frequently used for the $A + B$ problem but requires an appropriate generalization for the $A + A$ problem. Starting from this reaction-diffusion equation, we construct the first equations in a moment hierarchy whose first two members are the global density of A particles and the pair correlation function. We terminate the hierarchy via an approximation that relates the three-particle correlation function to two-particle correlation functions and thereby obtain a set of coupled equations that turns out to be linear and hence analytically tractable. This approach leads naturally to the proportionality of the rate of the reaction to the pair correlation function evaluated at $r = a$, where a is the diameter of the reacting particles. In other words, the reaction rate is proportional to the probability that two A particles are sufficiently close. In the more traditional approach based on the Smoluchowski theory for trapping phenomena, the reaction rate is instead proportional to the gradient of the pair correlation function. We discuss the differences between these points of view and their consequences. We also present numerical simulations in one and two dimensions in order to check our predictions. We confirm the well-known anomalous rate law in one dimension (the anomalies are marginal in two dimensions) and the proportionality of the reaction rate to the two-particle correlation function. Our simulations show that the rate of the reaction is indeed determined entirely by the spatial distribution of a very small shell of particles around a given reactant particle. Anomalous kinetics is a direct reflection of the deviation of the spatial distribution of this small shell from a random configuration. We also present simulation results that confirm the predicted distance and time scaling of the pair correlation function in one dimension.

I. Introduction

The diffusion-limited annihilation reaction $A + A \rightarrow$ products has been the subject of intense theoretical, numerical, and experimental study over the past decade.¹⁻⁷⁵ The "anomalous" behavior of this reaction in Euclidean dimensions $d \leq 2$ (and more generally in fractal systems of dimension $d_s \leq 2$, where d_s is the spectral dimension) is by now clearly established. These anomalies are apparent both in batch reactions,^{12-14,22-24,58,70-75} where one observes the decay of an initial distribution of A particles, and in steady-state reactions,^{5-21,38-40,46-53,58-59,65,74} where one continually supplies the system with A particles and one observes the characteristics of the steady state. In the batch reaction, the anomaly shows up most directly in the exponent X in the rate law $\dot{\rho} = -k\rho^X$, where $\rho(t)$ is the global density of A particles as a function of time. "Classical" chemical kinetics of well-stirred reactions yields an exponent $X = 2$, whereas the observed asymptotic rate law for this system yields $X = 1 + d_s/2$ for $d_s < 2$ with logarithmic corrections for $d_s = 2$. In the steady-state reaction, the anomaly is observed in the reaction law $Q = \rho_{ss}^X$, where Q is the rate at which A particles are continually injected in the system and ρ_{ss} is the steady-state density. Again, classical chemical kinetics yields $X = 2$, whereas the observed reaction law for the $A + A \rightarrow 0$ system is again $X = 1 + d_s/2$ for $d_s < 2$ with logarithmic corrections for $d_s = 2$. Note that the similarity in the behavior of the batch and steady-state exponents for the $A + A$ reaction contrasts

with the $A + B$ reaction, where the two behave quite differently and where even the critical dimensions for classical behavior are different for the two types of experiments.

It is by now well understood that rate laws are a direct reflection of the spatial distribution of particles. In particular, the classical rate law reflects a random Hertzian distribution, that is, one in which the probability that the nearest neighbor of a given particle is to be found at a distance r in a given direction peaks at $r = 0$ (suitably modified if the particles have a finite size). It is this continual supply of close pairs of particles even as they react that is embodied in the usual bimolecular rate law. Any form of thorough stirring ensures this supply;⁵⁶ diffusion in sufficiently high dimensions is such a thorough stirring mechanism. However, in low dimensions diffusion becomes ineffective. The anomalous rate laws are then a direct consequence of the deviation of the spatial distribution in these systems from a random one. Indeed, it is well established numerically that the distribution of particles in the $A + A$ system after long times in the batch reaction, or in the steady state, is almost latticelike in low Euclidean dimensions, with very few nearby pairs. The reaction thus slows down relative to its rate in the well-stirred system, and this slowing down is reflected in the higher exponents in the rate laws.

The anomalous behavior associated with the $A + A$ reaction is not merely of theoretical interest—indeed, it has been observed experimentally, some of the experiments having been carried out before the behavior was understood theoretically.^{50,75} Two kinds of $A + A$ experiments have been carried out that exhibit these effects: (1) exciton annihilation experiments in one-dimensional pores, in effectively one-dimensional isolated

* Permanent address: Department of Physics, University of Thessaloniki, GR-54006 Thessaloniki, Greece.

[⊗] Abstract published in *Advance ACS Abstracts*, May 1, 1995.

polymer wires, in fractal systems, and in ordinary three-dimensional systems,⁵⁰ and (2) excited molecule naphthalene fusion and quenching experiments in one-dimensional pores.⁷⁵ The anomalous effects are clearly seen in these experiments. Indeed, in ref 75 the discussion goes beyond the asymptotic rate laws that restricted earlier experimental analysis and deals with the spatial pattern formation of excitons and the effects of excitation time modulation on these spatial patterns.

Although the anomalous behaviors are now well understood qualitatively and numerically, the underlying theories are still not complete. Most of the theoretical arguments are based on scaling approaches that yield the correct exponents. Exact results for the A + A → products batch reaction have been obtained for one and two dimensions in the classic papers of Torney and McConnell⁶⁻⁸ and for one dimension also by Elyutin.¹⁶ For the steady-state problem an exact solution in one dimension was obtained by Racz²⁴ and also by Peacock-López and Keizer⁴³ on the basis of Keizer's general theory of fluctuations around the steady state. A related problem, the A + A → A "coagulation" reaction, has also been considered theoretically, numerically, and experimentally. This system has been solved asymptotically in one dimension by Spouge⁴⁶ and, more recently, for all times by Doering and Ben-Avraham,^{48,53} both for the batch reaction and the steady-state reaction.

The theoretical methods used in these approaches are powerful but rather specific in the sense that it is difficult to generalize them to problems other than the ones they were applied to. They include detailed enumeration of random walk paths by a few walkers and generalization to many walkers by induction methods (Torney and McConnell), interacting spinlike theories (Spouge), Ising modellike theories (Racz), and an elegant statement of the problem in terms of the dynamics of the interparticle separation instead of the particle densities (Doering and Ben-Avraham).

A theoretical approach that is appealing because of its generality is a reaction-diffusion formalism such as has been used extensively in the A + B → 0 problem.^{58,77-79} Herein we start from a generalized reaction-diffusion model for the A + A problem and obtain from it a hierarchy of equations involving increasing numbers of particles. This hierarchy is truncated at the two-particle level, and we solve the resulting set of equations to obtain the global density of A particles and also the spatial distribution as reflected in the pair correlation function. We apply our approach to both the batch reaction and the steady-state problem.

Our approach leads to a global reaction rate that is proportional to the pair correlation function; that is, the probability of a reaction is proportional to the probability that two A particles are located sufficiently near one another. This is to be contrasted with the more common Smoluchowski-type trapping boundary condition in which the probability of trapping is proportional to the gradient of the pair correlation function. We compare the results of these two viewpoints.

It may be helpful at this point to summarize briefly the historical development of the theory and its semantics. Originally, there were two distinct approaches to dealing with the chemical reaction term in the binary reaction problem. The first is essentially the law of mass action, where the reaction rate J is proportional to $\varrho_A\varrho_B$ or to ϱ_A^2 for an A + B or an A + A reaction, respectively. This is even now the most prevalent approach (see, e.g., Noyes' review⁷⁶) and employs the global time-dependent densities $\varrho(t)$ (the "macroscopic approach"). Within this same general viewpoint, recent ("microscopic") approaches have introduced the local densities $\varrho(\mathbf{r},t)$ instead (e.g., see refs 58 and 77-79). Historically, this microscopic approach goes back to Collins and Kimball,⁸⁰ even though their

contribution is intimately connected with the following (second) approach. The second approach, which we call the "extended Smoluchowski⁸¹ approach", was originally developed for the trapping of B particles on a stationary colloid A. It relates the reaction rate J to the instantaneous local flux of B particles across the boundary of the sphere determined by the capture radius a of the A particle. For a fixed diffusion constant D , Fick's First Law gives a linear relation between this flux and the radial component of the gradient on the boundary of the sphere, which we denote as $(\nabla\varrho)_{r=a}$. This Smoluchowski gradient approach needs to be augmented with an appropriate boundary condition for the density at the sphere boundary. The Smoluchowski boundary condition is $\varrho|_{r=a} = 0$. This results in the relation $J = D(\nabla\varrho)_{r=a}$ at long times. Svshnikoff⁸² generalized Smoluchowski's approach to probabilistic trapping (a sticking probability smaller than unity). On the basis of a hint by Smoluchowski,⁸¹ Svshnikoff also generalized the theory to ordinary bimolecular reactions where the size and diffusivity of A and B in the A + B → C reaction may be comparable. This generalization presents a number of problems originally stated by Collins and Kimball,⁸⁰ whose resolution of these problems led them to replace the Smoluchowski boundary condition by the relation between the reaction rate J and the local density at the boundary

$$J = k\varrho|_{r=a} \quad (1)$$

where k is a *microscopic rate constant* (representing, *inter alia*, the sticking coefficient). For instance, for the colloid it follows that for the B particles $\varrho|_{r=a}$ is linear with the radial component of the density gradient $\nabla\varrho$ at the boundary, i.e.,

$$\varrho|_{r=a} \sim (\nabla\varrho)_{r=a} \quad (2)$$

The so-called radiative boundary condition of Collins and Kimball (the name was actually given by Waite,⁸³ in analogy with the heat transfer problem) essentially combines the idea of the law of mass action with that of the Smoluchowski gradient. For the "symmetrized" ordinary bimolecular reaction, the difference between the Smoluchowski-Svshnikoff and the Collins and Kimball boundary conditions is best seen in the approach of Waite⁸³ and of Monchik et al.⁸⁴ This approach deals with the two-particle density $f(\mathbf{r},\mathbf{r}';t)$ and the boundary of the sphere of radius a is replaced by an interparticle distance a (still the capture radius) so that capture occurs when $\mathbf{r} = \mathbf{r}' + \mathbf{a}$, where \mathbf{a} has magnitude a and arbitrary direction. In the so-called generalized Smoluchowski approach the (absorptive) boundary condition is now

$$f(\mathbf{r},\mathbf{r}'=\mathbf{r}+\mathbf{a},t) = 0 \quad (3)$$

On the other hand, the generalized Collins and Kimball or radiative boundary condition requires that the Smoluchowski gradient be proportional to $f(\mathbf{r},\mathbf{r}'=\mathbf{r}+\mathbf{a},t)$, i.e.,

$$J \sim \langle (\nabla_{\mathbf{r}'} f(\mathbf{r},\mathbf{r}',t))_{\mathbf{r}'=\mathbf{r}+\mathbf{a}} \rangle \sim \langle f(\mathbf{r},\mathbf{r}'=\mathbf{r}+\mathbf{a},t) \rangle \quad (4)$$

where the subscript on the gradient operator denotes the variable with respect to which the gradient is to be taken and the brackets indicate normalized integrals over the position variables. Only for a random distribution is (4) equivalent to the macroscopic law of mass action,

$$J \sim \varrho_A(t)\varrho_B(t) \quad (5)$$

However, even a reactive system that starts from a random distribution deviates from randomness at longer times, especially

for interparticle distances of the order of a . It is interesting to note that for certain realistic limits, e.g., large k , the generalized Smoluchowski (absorptive boundary condition) and the Collins and Kimball (radiative boundary condition) approaches give identical answers.⁸⁰ Thus, little difference has been found between the two in the true diffusion-limited case in contrast to the so-called diffusion-controlled case, where the microscopic reaction ("sticking") probability is less than unity.

Following Waite⁸³ and Monchik et al.,⁸⁴ Wilemski and Fixman⁸⁵ have discussed in detail how to use "sink" (reaction) terms in the reaction-diffusion equation so as to derive the radiative (Waite) boundary condition for the two-particle density approach. Source terms were also added.⁸⁵ Further elaborations have been discussed by van Kampen,⁸⁶ de Gennes,⁸⁷ and Keizer.⁸⁸ The last two also discussed the problem for dimensions below three. In the literature the construction of the reaction (sink) term for the $A + A$ reaction problem seems to have been particularly problematic. Here we construct such a sink term, derive the generalized Collins and Kimball boundary condition,⁸³ and compare the results with those obtained with a Smoluchowski boundary condition. Furthermore, we do this for all integer dimensions.

In section II we present our reaction-diffusion model, obtain the first equations of the hierarchy implied by this model, and implement our approximation to break the hierarchy. The result is a closed set of equations for the global density of A particles and for the pair correlation function of the particles. In section III we solve these equations for a batch reaction, and in section IV we do so for the steady state in the presence of sources. Our simulation results are presented and discussed in section V. The comparison of our results with those obtained with a Smoluchowski boundary condition is presented in section VI. We end with a summary and some concluding remarks in section VII.

II. Reaction-Diffusion Model

We consider a d -dimensional Euclidean space on which A particles at an initial average density (number of particles per unit volume) ρ_0 diffuse freely. Two A particles annihilate, $A + A \rightarrow 0$, when they come in contact at a distance a between their centers (a is the "diameter" of each particle). We wish to calculate the rate law for the particles, that is, the law that governs the decay of the density $\rho(t)$ of A particles as a function of time. We also wish to calculate a measure of the interparticle separation that underlies the rate law.

A. Definitions. We formulate a reaction-diffusion model that leads to a hierarchy of equations involving, as usual, increasing numbers of particles at each level of the hierarchy. The hierarchy is constructed from a "microscopic" (albeit continuous) reaction-diffusion model and is truncated at the two-particle correlation function level. We show that this truncation leads to the known results for the $A + A$ problem. Although many of the results that we obtain are known from other approaches and from numerical simulations, our approach offers the advantage of arriving at all of these results within a single consistent point of view based on a single physically motivated approximation (truncation).

We begin by defining the local density $\rho(\mathbf{r}, t)$ of A particles at space point \mathbf{r} and time t ,

$$\rho(\mathbf{r}, t) \equiv \sum_i^{N(t)} \delta(\mathbf{r} - \mathbf{r}_i(t)) \quad (6)$$

where $\mathbf{r}_i(t)$ denotes the position of particle i at time t and $N(t)$ is the total number of particles in the system at time t . In terms of this local density, the average "one-particle" (global) density

introduced above is given by

$$\rho(t) \equiv N(t)/V \equiv \langle \rho(\mathbf{r}, t) \rangle_{\mathbf{r}} \quad (7)$$

Here V is the volume of the system. We also introduce the average two-particle density function

$$f(\mathbf{r}, t) \equiv \langle \rho(\mathbf{r}', t) \rho(\mathbf{r}' + \mathbf{r}, t) \rangle_{\mathbf{r}'} \quad (8)$$

and, similarly, the average three-particle density function

$$F(\mathbf{r}, \mathbf{r}', t) \equiv \langle \rho(\mathbf{r}'', t) \rho(\mathbf{r}'' + \mathbf{r}', t) \rho(\mathbf{r}'' + \mathbf{r}' + \mathbf{r}, t) \rangle_{\mathbf{r}''} \quad (9)$$

The definition of higher order averages is obvious but will not be needed. The subscripted brackets indicate an average over configuration space:

$$\langle F(\mathbf{r}') \rangle_{\mathbf{r}'} \equiv \frac{1}{V} \int d\mathbf{r}' F(\mathbf{r}') \quad (10)$$

The two-particle function by definition satisfies the identity

$$\langle f(\mathbf{r}, t) \rangle_{\mathbf{r}} = \frac{1}{V} \int d\mathbf{r} f(\mathbf{r}, t) = \rho^2(t) \quad (11)$$

For a random distribution of point particles $f(\mathbf{r}, t) = \rho^2(t)$ because the densities at different points are uncorrelated and hence the average of the product in (8) becomes simply the product of the averages. The three-particle density function satisfies the identities

$$\begin{aligned} \frac{1}{V} \int d\mathbf{r}' F(\mathbf{r}', \mathbf{r}'', t) &= \rho(t) f(\mathbf{r}'', t) \\ \frac{1}{V} \int d\mathbf{r}'' F(\mathbf{r}', \mathbf{r}'', t) &= \rho(t) f(\mathbf{r}', t) \\ \frac{1}{V^2} \int d\mathbf{r}' \int d\mathbf{r}'' F(\mathbf{r}', \mathbf{r}'', t) &= \rho^3(t) \end{aligned} \quad (12)$$

For a random distribution $f(\mathbf{r}, \mathbf{r}', t) = \rho^3(t)$. Our model for the $A + A$ reaction will ultimately depend only on the one-particle and two-particle density functions.

It is convenient to introduce the pair correlation function

$$g(\mathbf{r}, t) \equiv f(\mathbf{r}, t)/\rho^2(t) \quad (13)$$

This pair correlation function is of course normalized to unity,

$$\langle g(\mathbf{r}, t) \rangle_{\mathbf{r}} = \frac{1}{V} \int d\mathbf{r} g(\mathbf{r}, t) = 1 \quad (14)$$

and for a random distribution of point particles $g(\mathbf{r}, t) = 1$. Similarly, the three-particle correlation function is defined by

$$G(\mathbf{r}, \mathbf{r}', t) \equiv F(\mathbf{r}, \mathbf{r}', t)/\rho^3(t) \quad (15)$$

and is also normalized to unity, $\langle\langle G(\mathbf{r}, \mathbf{r}', t) \rangle\rangle_{\mathbf{r}, \mathbf{r}'} = 1$.

B. Reaction-Diffusion Equation. Our model starts with a reaction-diffusion equation for the local density from which we then construct an equation for the average density, for the two-particle density function, etc. In the $A + B$ problem with local densities $\rho_A(\mathbf{r}, t)$ and $\rho_B(\mathbf{r}, t)$ the reaction-diffusion equation ubiquitously used in the literature is⁷⁷⁻⁷⁹

$$\frac{\partial}{\partial t} \rho_A(\mathbf{r}, t) = D \nabla^2 \rho_A(\mathbf{r}, t) - k \rho_A(\mathbf{r}, t) \rho_B(\mathbf{r}, t) + Q_A(\mathbf{r}, t) \quad (16)$$

and similarly for $\rho_B(\mathbf{r}, t)$, where D is the diffusion coefficient (often assumed to be equal for both species), k is a local reaction

rate coefficient, and $Q_A(\mathbf{r}, t)$ is a source term modeling external sources if the system is open. In the case of a single species this model is usually abandoned because a reaction term of the form $-k\rho^2(\mathbf{r}, t)$ does not distinguish between the reaction of two different A particles or of a single A particle inappropriately reacting "with itself". Therefore, while a great deal of the AB literature starts from eq 16, the starting point for the AA literature is usually quite different. We wish to formulate a model that starts from the same sort of formulation as (16) but is suitably adjusted to the AA case.

A physically motivated adjustment is provided by the generalized reaction-diffusion equation⁵⁸

$$\frac{\partial}{\partial t} \rho(\mathbf{r}, t) = D\nabla^2 \rho(\mathbf{r}, t) - k \int d\mathbf{R} \rho(\mathbf{r}, t) \rho(\mathbf{r}+\mathbf{R}, t) \delta(R-a) + Q(\mathbf{r}, t) \quad (17)$$

This equation says that the local density of A's changes through diffusion, through the reaction of the A particle in question with another A particle a distance a away from it, and through external sources. Equation 17 is not the usual local equation, but that is the price that must be paid to deal with the A + A reaction in this language. Equation 17 is our basic model, with the further restriction that we will here only consider space-independent sources, $Q(\mathbf{r}, t) = Q(t)$. In writing such continuum models, one usually has in mind (and one usually simulates when dealing with such systems numerically) an underlying discrete lattice of lattice constant a in which A particles hop from site to a site with a hopping rate Γ . The continuum limit is strictly appropriate as $a \rightarrow 0$ and $\Gamma \rightarrow \infty$ in such a way that $D \equiv \Gamma a^2/Z_d$ is finite. Here Z_d is the number of nearest neighbors of any site.

C. Rate Equation for the Average Particle Density. The evolution equation for the global density $\rho(t)$ is obtained by integrating (17) over \mathbf{r} and dividing by the volume. With the definitions (7), (8), and (13) we find

$$\begin{aligned} \dot{\rho}(t) &= -k \int d\mathbf{R} f(\mathbf{R}, t) \delta(R-a) + Q(t) \\ &= -k\Omega_d a^{d-1} f(a, t) + Q(t) \\ &= -k\Omega_d a^{d-1} \rho^2(t) g(a, t) + Q(t) \end{aligned} \quad (18)$$

where the dot denotes a time derivative and Ω_d is the solid angle in d dimensions. Note the dependence of the reaction term on the pair correlation function.⁸⁶ We have implemented statistical spatial isotropy and the consequent dependence of $f(\mathbf{r}, t)$ only on $|\mathbf{r}| = r$ and not on angles. Here and subsequently we simply replace a vectorial argument by a scalar argument, $h(\mathbf{r}) = h(r)$, when a function is known not to depend on the orientation of \mathbf{r} . Equation 18 is the first equation in a hierarchy.

Equation 18 is of the standard form

$$\dot{\rho}(t) = Q(t) - J(t) \quad (19)$$

where the injection rate per unit volume $Q(t)$ is zero for a batch reaction and where $J(t)$ is the reaction term, which in our model is proportional to the pair correlation function,

$$J(t) = -k\Omega_d a^{d-1} \rho^2(t) g(a, t) = -k\Omega_d a^{d-1} f(a, t) \quad (20)$$

The rate law (19) is of the standard classical bimolecular form if the pair correlation function $g(a, t)$ is independent of time. "Anomalous" behavior is therefore reflected in the time dependence of the pair correlation function.

D. Rate Equation for the Pair Correlation Function. The second equation in the hierarchy is that of the two-particle

density function or of the pair correlation function. To construct this equation consider the rate of change of the product of two densities:

$$\frac{d}{dt} [\rho(\mathbf{r}, t) \rho(\mathbf{r}+\mathbf{r}', t)] = \dot{\rho}(\mathbf{r}, t) \rho(\mathbf{r}+\mathbf{r}', t) + \rho(\mathbf{r}, t) \dot{\rho}(\mathbf{r}+\mathbf{r}', t) - k\rho(\mathbf{r}, t) \rho(\mathbf{r}+\mathbf{r}', t) \delta(r'-a) \quad (21)$$

The derivative on the left represents all the different ways in which this product can change. The first two terms on the right represent the possible changes in each of the two densities in the product due to diffusion and due to the reaction of a particle at \mathbf{r} with a third particle and of a particle at \mathbf{r}' with a third particle. The $\dot{\rho}$'s in these two terms are thus given by (17). The last term on the right represents the direct reaction of the two particles in question, the one at \mathbf{r} and the one at $\mathbf{r} + \mathbf{r}'$. Substituting (17) into (21) yields

$$\begin{aligned} \frac{\partial}{\partial t} [\rho(\mathbf{r}, t) \rho(\mathbf{r}+\mathbf{r}', t)] &= -k\rho(\mathbf{r}, t) \rho(\mathbf{r}+\mathbf{r}', t) \delta(r'-a) + \\ &\rho(\mathbf{r}+\mathbf{r}', t) (D\nabla_{\mathbf{r}}^2 \rho(\mathbf{r}, t) - k \int d\mathbf{R} \rho(\mathbf{r}, t) \rho(\mathbf{r}+\mathbf{R}, t) \delta(R-a) + \\ &Q(t)) + \rho(\mathbf{r}, t) (D\nabla_{\mathbf{r}+\mathbf{r}'}^2 \rho(\mathbf{r}+\mathbf{r}', t) - k \int d\mathbf{R} \rho(\mathbf{r}+\mathbf{r}', t) \times \\ &\rho(\mathbf{r}+\mathbf{r}'+\mathbf{R}, t) \delta(R-a) + Q(t)) \end{aligned} \quad (22)$$

The subscripts on the operators ∇^2 indicate the variable with respect to which these operators are to be evaluated.

The next step is to integrate (22) over \mathbf{r} and divide by V . We obtain⁸⁶

$$\begin{aligned} \dot{f}(r', t) &= -kf(r', t) \delta(r'-a) + \frac{D}{V} \int d\mathbf{r} (\rho(\mathbf{r}+\mathbf{r}', t) \nabla_{\mathbf{r}}^2 \rho(\mathbf{r}, t) + \\ &\rho(\mathbf{r}, t) \nabla_{\mathbf{r}+\mathbf{r}'}^2 \rho(\mathbf{r}+\mathbf{r}', t)) - k \int d\mathbf{R} \delta(R-a) (F(\mathbf{r}', \mathbf{R}, t) + \\ &F(-\mathbf{r}', \mathbf{R}, t)) + 2Q(t) \rho(t) \end{aligned} \quad (23)$$

The second term on the right can be integrated by parts twice, and the derivatives with respect to \mathbf{r} can be converted to derivatives with respect to \mathbf{r}' so that we can write

$$\begin{aligned} \frac{D}{V} \int d\mathbf{r} \rho(\mathbf{r}+\mathbf{r}', t) \nabla_{\mathbf{r}}^2 \rho(\mathbf{r}, t) &= \frac{D}{V} \int d\mathbf{r} [\nabla_{\mathbf{r}'}^2 \rho(\mathbf{r}+\mathbf{r}', t)] \rho(\mathbf{r}, t) \\ &= \frac{D}{V} \int d\mathbf{r} \nabla_{\mathbf{r}'}^2 \rho(\mathbf{r}+\mathbf{r}', t) \rho(\mathbf{r}, t) = D\nabla_{\mathbf{r}'}^2 f(r', t) \end{aligned} \quad (24)$$

The third term on the right of (23) can be dealt with similarly:

$$\begin{aligned} \frac{D}{V} \int d\mathbf{r} \rho(\mathbf{r}, t) \nabla_{\mathbf{r}+\mathbf{r}'}^2 \rho(\mathbf{r}+\mathbf{r}', t) &= \frac{D}{V} \int d\mathbf{r} \rho(\mathbf{r}, t) \nabla_{\mathbf{r}'}^2 \rho(\mathbf{r}+\mathbf{r}', t) \\ &= D\nabla_{\mathbf{r}'}^2 f(r', t) \end{aligned} \quad (25)$$

Combining these results in (23), we then have

$$\begin{aligned} \dot{f}(r', t) &= -kf(r', t) \delta(r'-a) + 2D\nabla_{\mathbf{r}'}^2 f(r', t) - \\ &k \int d\mathbf{R} \delta(R-a) [F(\mathbf{r}', \mathbf{R}, t) + F(-\mathbf{r}', \mathbf{R}, t)] + 2Q(t) \rho(t) \end{aligned} \quad (26)$$

This equation is an exact consequence of our starting model—no further approximations have yet been made. Its consistency with (18) can be checked by integrating over \mathbf{r}' and dividing by $2V\rho(t)$. In the thermodynamic limit ($V \rightarrow \infty$), the first term on the right does not contribute to this integrated expression and (18) is recovered.

It is more convenient to write (26) in terms of the pair correlation function $g = f/\rho^2$ and the three particle correlation function $G = F/\rho^3$. These substitutions followed by division by $\rho^2(t)$ (and relabeling \mathbf{r}' as \mathbf{r}) immediately gives

$$2\frac{\dot{\rho}(t)}{\rho(t)}g(\mathbf{r},t) + \dot{g}(\mathbf{r},t) = -kg(\mathbf{r},t)\delta(r-a) + 2D\nabla^2g(\mathbf{r},t) + \frac{2Q(t)}{\rho(t)} - k\rho(t)\int d\mathbf{R}\delta(R-a)[G(\mathbf{r},\mathbf{R},t) + G(-\mathbf{r},\mathbf{R},t)] \quad (27)$$

This is the second equation in our hierarchy.

E. Breaking the Hierarchy: Two-Particle Approximation.

Our approximation to break the hierarchy consists of writing the three-particle correlation function as a product of two two-particle correlation functions:

$$G(\mathbf{r},\mathbf{R},t) \approx g(\mathbf{r},t)g(\mathbf{R},t) \quad (28)$$

Thus, the probability of a triplet of particles separated by \mathbf{r} and \mathbf{R} (and $\mathbf{r} + \mathbf{R}$) is written as the product of the probabilities of a pair separated by \mathbf{r} and another pair separated by \mathbf{R} . Note that (28) preserves the correct normalization to unity for $G(\mathbf{r},\mathbf{R},t)$. We further note the two identities $g(-\mathbf{r},t) = g(\mathbf{r},t)$ and

$$\int d\mathbf{R}\delta(R-a)g(\mathbf{R},t) = \Omega_d a^{d-1}g(a,t) \quad (29)$$

and recall the rate equation (18) so that

$$-k\Omega_d a^{d-1}g(a,t) = \frac{\dot{\rho}(t)}{\rho^2(t)} - \frac{Q(t)}{\rho^2(t)} \quad (30)$$

Substitution of (28)–(30) into (27) then yields the much simpler equation

$$\dot{g}(\mathbf{r},t) = 2D\nabla^2g(\mathbf{r},t) - kg(\mathbf{r},t)\delta(r-a) + 2\frac{Q(t)}{\rho(t)}[1 - g(\mathbf{r},t)] \quad (31)$$

Equation 31 together with the rate equation (18)

$$\dot{\rho}(t) = -k\Omega_d a^{d-1}g(a,t)\rho^2(t) + Q(t) \quad (32)$$

then constitute our closed set of equations.

We can write (32) in the form

$$\dot{\rho}(t) = -k(t)\rho^2(t) + Q(t) \quad (33)$$

where $k(t)$ is the effective rate coefficient for the reaction

$$k(t) = -k\Omega_d a^{d-1}g(a,t) \quad (34)$$

If $g(a,t)$ is asymptotically constant, then (33) is asymptotically an ordinary second order rate law that leads to the usual classical results for well-stirred reactions. If, on the other hand, $g(a,t)$ turns out to be time-dependent at long times, then the rate law is “anomalous”. If our theory is correct, then we should find that $g(a,t)$ is asymptotically time-dependent (proportional to $t^{-d/2}$) for $d < 2$ and time-independent for $d > 2$ ($d = 2$ should be the critical dimension). An alternate way to write eq 33 is⁵⁰

$$\dot{\rho}(t) = -k'\rho^X(t) + Q(t) \quad (35)$$

where k' is a constant independent of time and where anomalous behavior is reflected in deviations of the exponent X from the classical value $X = 2$. This leads to the more physical representation of (33)

$$\dot{\rho}(t) = -k(\rho)\rho^2(t) + Q(t) \quad (36)$$

thus recognizing that anomalies are reflected in the density dependence of the effective rate coefficient.

The classical vs anomalous behavior of the system should also become apparent in the asymptotic behavior of the pair

correlation function. If the system behaves classically, then the spatial distribution of particles should become essentially random and $g(\mathbf{r},t)$ should approach 1 at long times independent of \mathbf{r} (except for small corrections due to the finite radius a of the particles). Anomalous behavior is associated with a deviation from this uniform distribution, a deviation that persists even in the limit $a \rightarrow 0$. Indeed, simulations⁸⁹ show that for $d < 2$ there is a dearth of near neighbors surrounding any given particle, and it is this depletion that causes the reaction to slow down. This depletion should show up in a decrease of $g(\mathbf{r},t)$ as a function of r as $r \rightarrow 0$. We expect to find such behavior for $d < 2$, while for $d > 2$ the pair correlation function is expected to be essentially constant.

An important point needs to be made here concerning the truncation of (27). Van Kampen⁸⁶ discusses the $A + A$ reaction and associated cluster expansions and makes the important assertion that *the only systematic way to arrive at an approximate solution is to expand in powers of a parameter*. He cautions against truncating the hierarchy on intuitive grounds, finding such intuitive approaches to be unreliable. One possible expansion parameter is the particle density (van Kampen discusses the equivalence of dealing with the initial particle density or the density as a function of time), and in this context he specifically addresses eq 27. His conclusions regarding the order in density of the different terms in (27) are based on the assumption that the pair correlation function is of $O(1)$ in the density (van Kampen does *not* address low-dimensional systems; this assumption is therefore correct in his discussion). This leads to the conclusion that the first term on the left of (27) and the last term on the right are of higher order in the density than are the remaining terms (he only considers batch reactions) and should therefore be dropped in a theory that deals only with leading order behavior in the density. In other words, he argues that the precise cancellation of these terms, which arises as a result of the hierarchy breakage (28), is irrelevant since both of these terms should be dropped anyway. We note here that this argument does *not* carry through in any straightforward way when the behavior of the system is anomalous since the pair correlation function itself becomes density-dependent. *Ex post* it will turn out that these two terms are indeed of lower order in the $A + A$ problem even in low dimensions (but *not* in the $A + B$ problem), but this cannot be deduced *ex ante*. Indeed, the assumption we have made here is only justified *ex post* by its success, and therefore it can be argued that simply dropping the two “cancelling” terms is an equally reasonable assumption.

We end this section by writing, for comparison, the equations that would replace (31) and (32) in a Smoluchowski-type approach (see the Introduction). In this more traditional approach the reaction terms are chosen according to the “Smoluchowski boundary condition” derived for diffusion-limited trapping processes (see, e.g., ref 59)

$$\dot{\rho}(t) = Q(t) - J_S(t) \quad (37)$$

but now

$$J_S(t) = 2D \int d\mathbf{r} \frac{\partial}{\partial r} f(\mathbf{r},t) \delta(r-a) = 2D\Omega_d a^{d-1} \rho^2(t) \left. \frac{\partial}{\partial r} g(r,t) \right|_{r=a} \quad (38)$$

that is, the gradient of the pair correlation function rather than the pair correlation function itself drives the reaction. The factor of 2 in (38) reflects the disappearance of two A particles upon reaction. Our description (19) with (20) seems more appropriate for the $A + A$ reaction.

We note that in the Smoluchowski approach there is no separate “local reaction rate coefficient” k since the reaction

term now arises as a consequence of a trapping boundary condition. The Smoluchowski rate coefficient is related to the diffusion coefficient by

$$k = 2D/a \quad (39)$$

where a is the radius of the trap.

If one follows a procedure similar to the one we followed to truncate our hierarchy but with the Smoluchowski reaction term, one finds for the second equation of the hierarchy

$$\dot{g}(\mathbf{r}, t) = 2D\nabla^2 g(\mathbf{r}, t) - 2D \left[\frac{\partial}{\partial r} g(\mathbf{r}, t) \right] \delta(r-a) + 2 \frac{Q(t)}{Q(t)} [1 - g(\mathbf{r}, t)] \quad (40)$$

in place of (31). In the Smoluchowski approach one imposes, in addition, the absorbing boundary condition (inconsistent with our approach) that

$$f(a, t) = g(a, t) = 0 \quad (41)$$

We will discuss the comparison of the solution of this hierarchy with our method in section VI.

III. Batch Reactions

We begin by considering batch reactions, that is, reactions in which there is no source other than the initial distribution of A particles ($Q = 0$). Our two hierarchy equations (32) and (31) then reduce to

$$\dot{\varrho}(t) = -k\Omega_d a^{d-1} g(a, t) \varrho^2(t) \quad (42)$$

$$\begin{aligned} \dot{g}(\mathbf{r}, t) &= 2D\nabla^2 g(\mathbf{r}, t) - kg(\mathbf{r}, t) \delta(r-a) \\ &= 2D\nabla^2 g(\mathbf{r}, t) - kg(a, t) \delta(r-a) \end{aligned} \quad (43)$$

Equation 43 is a linear equation that can easily be solved by Fourier-Laplace transformation. We first Fourier transform according to

$$\hat{g}_{\mathbf{n}}(t) = \frac{1}{L^{d/2}} \int d\mathbf{r} g(\mathbf{r}, t) e^{-2i\pi\mathbf{n}\cdot\mathbf{r}/L} \quad (44)$$

where $L^d = V$, the system volume, and \mathbf{n} is the d -tuple of integers n_1, n_2, \dots, n_d . The inverse transformation is

$$g(\mathbf{r}, t) = \frac{1}{L^{d/2}} \sum_{n_1, \dots, n_d = -\infty}^{\infty} \hat{g}_{\mathbf{n}}(t) e^{2i\pi\mathbf{n}\cdot\mathbf{r}/L} \quad (45)$$

In writing (44) and (45), we have assumed periodic boundary conditions. Transformation of (43) according to (44) yields

$$\dot{\hat{g}}_{\mathbf{n}}(t) = -\frac{8D\pi^2}{L^2} n^2 \hat{g}_{\mathbf{n}}(t) - kg(a, t) H_{d, \mathbf{n}} \quad (46)$$

where

$$H_{1, \mathbf{n}} = \frac{2}{L^{1/2}} \cos(2\pi\mathbf{n}a/L) \quad (47)$$

$$H_{2, \mathbf{n}} = \frac{2\pi a}{L} J_0(2\pi\mathbf{n}a/L) \quad (48)$$

$$H_{3, \mathbf{n}} = \frac{4\pi a^2}{L^{3/2}} \left(\frac{\sin(2\pi\mathbf{n}a/L)}{2\pi\mathbf{n}a/L} \right) \quad (49)$$

$J_0(z)$ is a Bessel function of the first kind. The ordinary

differential equation (46) has the solution

$$\hat{g}_{\mathbf{n}}(t) = e^{-(8D\pi^2 n^2/L^2)t} \hat{g}_{\mathbf{n}}(0) - k \int_0^t dt' g(a, t') \hat{K}_{d, \mathbf{n}}(t-t') \quad (50)$$

where

$$\hat{g}_{\mathbf{n}}(0) = \frac{1}{L^{d/2}} \int d\mathbf{r} g(\mathbf{r}, 0) e^{-2i\pi\mathbf{n}\cdot\mathbf{r}/L} \quad (51)$$

$$\hat{K}_{d, \mathbf{n}}(t) = H_{d, \mathbf{n}} e^{-(8D\pi^2 n^2/L^2)t} \quad (52)$$

The inverse Fourier transform of (50) is

$$g(\mathbf{r}, t) = g_0(\mathbf{r}, t) - k \int_0^t dt' g(a, t') K_d(\mathbf{r}, t-t') \quad (53)$$

where

$$g_0(\mathbf{r}, t) = \frac{1}{L^{d/2}} \sum_{n_1, \dots, n_d = -\infty}^{\infty} \hat{g}_{\mathbf{n}}(0) e^{-(8D\pi^2 n^2/L^2)t} e^{2i\pi\mathbf{n}\cdot\mathbf{r}/L} \quad (54)$$

is the pair correlation function for a purely diffusive process, that is, in the absence of any reactions, and

$$K_d(\mathbf{r}, t) = \frac{1}{L^{d/2}} \sum_{n_1, \dots, n_d = -\infty}^{\infty} \hat{K}_{d, \mathbf{n}}(t) e^{2i\pi\mathbf{n}\cdot\mathbf{r}/L} \quad (55)$$

Since (53) is a convolution, its time Laplace transform according to

$$\tilde{F}(s) = \int_0^{\infty} dt e^{-st} F(t) \quad (56)$$

is particularly simple and useful:

$$\tilde{g}(\mathbf{r}, s) = \tilde{g}_0(\mathbf{r}, s) - k\tilde{g}(a, s) \tilde{K}_d(\mathbf{r}, s) \quad (57)$$

With (51) in (54) we find

$$\begin{aligned} g_0(\mathbf{r}, t) &= \frac{1}{L^d} \sum_{\mathbf{n}} \int d\mathbf{r}' g(\mathbf{r}', 0) e^{-2i\pi\mathbf{n}\cdot(\mathbf{r}'-\mathbf{r})/L} e^{-(8D\pi^2 n^2/L^2)t} \\ &\equiv \sum_{\mathbf{n}} g_{0, \mathbf{n}}(\mathbf{r}, t) \end{aligned} \quad (58)$$

The $\mathbf{n} = \mathbf{0}$ term in (58) is fixed by (14) regardless of the size of the system:

$$g_{0, \mathbf{0}}(\mathbf{r}, t) = \frac{1}{V} \int d\mathbf{r}' g(\mathbf{r}', 0) = 1 \quad (59)$$

This \mathbf{r} -independent nondecaying contribution dominates the long-time behavior of $g_0(\mathbf{r}, t)$ since all the other contributions decay with time. Indeed, if the initial distribution is uniform *without regard to the finite size of the particles*, then $g(\mathbf{r}, 0) = 1$ and $g_0(\mathbf{r}, t)$ remains exactly equal to unity for all time. If we are only interested in the long-time behavior of the particle density, then we retain only the Laplace transform of the nondecaying contribution, i.e., we set

$$\tilde{g}_0(\mathbf{r}, s) \sim 1/s \quad (60)$$

(to obtain the short-time behavior, we need to specify the initial condition in detail).

Now consider the second term of (53). The function $K_d(\mathbf{r}, t)$ decays with time (the only possibly nondecaying contribution

is the $\mathbf{n} = 0$ term in the sum, which vanishes in the thermodynamic limit). In the large-volume limit the sum in (55) can thus be replaced by the integral

$$K_d(\mathbf{r}, t) = \frac{1}{(2\pi)^{d/2}} \int d\mathbf{q} e^{i\mathbf{q}\cdot\mathbf{r}} e^{-2Dq^2 t} H_d(\mathbf{q}) \quad (61)$$

where

$$H_1(q) = \frac{2}{(2\pi)^{1/2}} \cos(qa) \quad (62)$$

$$H_2(\mathbf{q}) = \frac{2\pi a}{(2\pi)} J_0(qa) \quad (63)$$

$$H_3(\mathbf{q}) = \frac{4\pi a^2}{(2\pi)^{3/2}} \frac{\sin(qa)}{qa} \quad (64)$$

(Note that the sum (58) can only be approximated by an integral in the $V \rightarrow \infty$ limit *after* the nondecaying $\mathbf{n} = 0$ contribution has been explicitly separated; otherwise this all-important contribution would get lost in the limit.)

Equation 57 (or, more precisely, its integral over angles) can now be used to solve for the unknown quantity $g(a, t)$ that appears on the right hand side of (57) by setting $r = a$:

$$\tilde{g}(a, s) = \tilde{g}_0(a, s) - k\tilde{g}(a, s) \tilde{K}_d(a, s) \quad (65)$$

so that

$$\tilde{g}(a, s) = \frac{\tilde{g}_0(a, s)}{1 + k\tilde{K}_d(a, s)} \quad (66)$$

In view of the discussion surrounding (60) we immediately observe that the long-time behavior of $g(a, t)$ *regardless of initial condition* (and indeed its behavior for all time for a uniform initial condition) is obtained from

$$\tilde{g}(a, s) = \frac{1}{s[1 + k\tilde{K}_d(a, s)]} \quad (67)$$

Finally, the Laplace transform of the pair correlation function according to (57) then is

$$\tilde{g}(r, s) = \tilde{g}_0(r, s) - \frac{k\tilde{g}_0(a, s) \tilde{K}_d(r, s)}{k\tilde{K}_d(a, s) + 1} \quad (68)$$

Further discussion requires that we evaluate the functions K_d explicitly, which in turn must be done separately for each dimension.

A. One Dimension. In one dimension we find (with $r = |x|$, where x is the usual Cartesian coordinate)

$$K_1(r, t) = \frac{1}{2(2\pi Dt)^{1/2}} [e^{-(r-a)^2/8Dt} + e^{-(r+a)^2/8Dt}] \quad (69)$$

The Laplace transform of $K_1(r, t)$ is

$$\tilde{K}_1(r, s) = \frac{1}{2(2Ds)^{1/2}} [e^{-(s/2D)^{1/2}|r-a|} + e^{-(s/2D)^{1/2}|r+a|}] \quad (70)$$

Setting $r = a$ and substituting into (67), we obtain

$$\tilde{g}(a, s) = \frac{1}{s + [ks^{1/2}/2(2D)^{1/2}][1 + e^{-(2s/D)^{1/2}a}]} \quad (71)$$

and therefore for small s

$$\tilde{g}(a, s) \sim \frac{(2D)^{1/2}}{ks^{1/2}} + \frac{2D - ka}{k^2} + O(s^{1/2}) \sim \frac{(2D)^{1/2}}{ks^{1/2}} \quad (72)$$

The inverse transform of (72) is

$$g(a, t) \sim \frac{(2D)^{1/2}}{k(\pi t)^{1/2}} \quad (73)$$

This immediately gives for (42) with $d = 1$ and $\Omega_1 = 2$

$$\dot{\varrho}(t) = -2 \frac{(2D)^{1/2}}{(\pi t)^{1/2}} \varrho^2(t) \quad (74)$$

that is, a rate coefficient asymptotically proportional to $t^{-1/2}$. From (74) we easily deduce that

$$\varrho(t) = \frac{1}{4} \left(\frac{\pi}{2D} \right)^{1/2} t^{-1/2} \quad (75)$$

and consequently

$$\dot{\varrho} = - \frac{16D}{\pi} \varrho^3 \quad (76)$$

Such an asymptotic third-order rate law in one dimension has been found with use of a variety of other approaches and also from simulations. Note that the rate coefficient is entirely determined by the diffusion coefficient D and is otherwise independent of the size a of the particles and of the local rate coefficient k . This observation is also borne out by numerical simulations.

The spatial distribution of reactants is now found from (68). It simplifies the final results to note that for diffusion-controlled reactions k is large (e.g., eq 39) in the sense that $kK_1(a, s) \sim k/(2Ds)^{1/2} \gg 1$ except for very large values of s (which only affects the shortest time behavior). We thus set

$$\tilde{g}(r, s) \sim \frac{1}{s} \left(1 - \frac{\tilde{K}_1(r, s)}{\tilde{K}_1(a, s)} \right) \quad (77)$$

Further, again no important physical information is lost by setting $a = 0$ in this expression—as in the rate law, the finite size of the particles here does not play an important role. We then have

$$\tilde{g}(r, s) \sim \frac{1}{s} (1 - e^{-(s/2D)^{1/2}r}) \quad (78)$$

whose inverse Laplace transform is

$$g(r, t) = \text{erf} \left(\frac{r}{2(2Dt)^{1/2}} \right) \quad (79)$$

This expression is exactly of the desired form: at large values of r , $g(r, t) \rightarrow 1$; that is, there is no long-range order in the system. For small r , however, there is definite structure in the pair correlation function. A depletion region around each reactant particle grows in time as $t^{1/2}$. Note also that this result preserves the correct normalization of $g(r, t)$.

B. Two Dimensions. In two dimensions we obtain

$$\begin{aligned} \tilde{K}_2(r, s) &= \frac{a}{2\pi} \int d\mathbf{q} e^{i\mathbf{q}\cdot\mathbf{r}} \frac{1}{2Dq^2 + s} J_0(qa) \\ &= a \int_0^\infty dq \frac{q}{2Dq^2 + s} J_0(qr) J_0(qa) \end{aligned}$$

$$= \frac{a}{2D} I_0(a(s/2D)^{1/2}) K_0(r(s/2D)^{1/2}) \quad (80)$$

where I_0 and K_0 are modified Bessel functions and $r \geq a$. For small s one obtains

$$\tilde{K}_2(r,s) \sim \frac{a}{2D} \left[\ln 2 - \gamma - \frac{1}{2} \left(\frac{r^2 s}{2D} \right) \right] \quad (81)$$

where $\gamma = 0.577\dots$ is the Euler constant. The leading contribution in s to $\tilde{g}(r,s)$ is

$$\tilde{g}(r,s) \sim - \frac{4D}{kas \ln(r^2 s/2D)} \quad (82)$$

In the absence of the logarithmic term in the denominator we would find that $g(a,t)$ is approximately constant independent of t (cf. next subsection for three dimensions) and an associated classical rate law $\dot{c} \sim -c^2$. The logarithmic contribution leads to the well-known logarithmic reduction to the classical rate law in two dimensions and to logarithmic deviations from a uniform spatial pair correlation function.

C. Three Dimensions. In three dimensions we readily find

$$\begin{aligned} K_3(r,t) &= \frac{4\pi a^2}{(2\pi)^3} \int d\mathbf{q} e^{i\mathbf{q}\cdot\mathbf{r}} e^{-2Dq^2 t} \sin(qa)/qa \\ &= \frac{a}{2r} \frac{1}{(2\pi Dt)^{1/2}} [e^{-(a-r)^2/8Dt} - e^{-(a+r)^2/8Dt}] \end{aligned} \quad (83)$$

The Laplace transform of $K_3(r,t)$ then is

$$\tilde{K}_3(r,s) = \frac{a}{2r} \frac{1}{(2D)^{1/2}} \frac{1}{s^{1/2}} [e^{-(s/2D)^{1/2}|r-a|} - e^{-(s/2D)^{1/2}|r+a|}] \quad (84)$$

Setting $r = a$, we find

$$\tilde{K}_3(a,s) = \frac{1}{2(2Ds)^{1/2}} [1 - e^{-(2sD)^{1/2}a}] \quad (85)$$

and, for small s ,

$$\tilde{K}_3(a,s) \sim \frac{a}{2D} + O(s^{1/2}) \quad (86)$$

Substituting (85) into (67), we obtain

$$\tilde{g}(a,s) = \frac{1}{s + k(s/8D)^{1/2} [1 - e^{-(2sD)^{1/2}a}]} \quad (87)$$

and therefore for small s

$$\tilde{g}(a,s) \sim \frac{1}{s + (1 + ka/2D)} + O(s^{-1/2}) \quad (88)$$

The inverse transform of (88) is

$$g(a,t) \sim \frac{1}{1 + ka/2D} \quad (89)$$

that is, a constant rate coefficient for long times. Equation 42 with $d = 3$ and $\Omega_d = 4\pi$ then yields the classical rate law

$$\dot{c} = - \frac{4\pi a^2 k}{1 + ka/2D} c^2 \quad (90)$$

If we set $k = 2D/a$ as in (39), we have

$$\dot{c} = -4\pi Da c^2 \quad (91)$$

Note that the rate coefficient depends explicitly on the size a of the particles and that there is no reaction if the particles are point particles.

The spatial distribution of reactants is found from (68):

$$\begin{aligned} \tilde{g}(r,s) &\sim \frac{1}{s} \left(1 - \frac{k\tilde{K}_3(r,s)}{k\tilde{K}_3(a,s) + (a/2D)} \right) \sim \\ &\frac{1}{s} \left[1 - \left(\frac{ka}{2r(2Ds)^{1/2}} (e^{-(s/2D)^{1/2}|r-a|} - e^{-(s/2D)^{1/2}|r+a|}) \right) \right. \\ &\quad \left. \left(\frac{k}{2(2Ds)^{1/2}} (1 - e^{-2(s/2D)^{1/2}a}) + 1 \right) \right] \end{aligned} \quad (92)$$

For $(s/2D)^{1/2}a \ll 1$, $k/2Ds \gg 1$, and $a \leq r$ this reduces to

$$\tilde{g}(r,s) \sim \frac{1}{s} \left[1 - \frac{a}{r(1 + 2D/ka)} e^{-(s/2D)^{1/2}r} \right] \quad (93)$$

and inverse Laplace transformation of this expression immediately yields

$$g(r,t) \sim 1 - \frac{a}{r(1 + 2D/ka)} \operatorname{erfc} \left(\frac{r}{2(2Dt)^{1/2}} \right) \quad (94)$$

The spatial distribution thus approaches a uniform one (except for corrections of order a) and indeed remains uniform for all time if $a = 0$. If we set $k = 2D/a$, we have the even simpler form

$$g(r,t) \sim 1 - \frac{a}{2r} \operatorname{erfc} \left(\frac{r}{2(2Dt)^{1/2}} \right) \quad (95)$$

In any case, there is no growing depletion zone. This result is of course well-known from numerical simulations.

IV. Steady-State Reactions

In this section we consider the steady state when there are sources present, that is, when $Q \neq 0$ and $\dot{c} = 0$. Our two hierarchy equations (32) and (31) then become

$$Q = k\Omega_d a^{d-1} c^2 g(a) \quad (96)$$

$$0 = 2D\nabla^2 g(\mathbf{r}) - kg(\mathbf{r}) \delta(r-a) + \frac{2Q}{c} [1 - g(\mathbf{r})] \quad (97)$$

where the absence of a time argument where there was one previously denotes the steady state.

As before, we Fourier transform (97) according to (44) to obtain

$$0 = - \frac{8D\pi^2}{L^2} n^2 \hat{g}_n - \frac{Q}{\Omega_d a^{d-1} c^2} H_{d,n} + \frac{2Q}{c} [L^{d/2} \delta_{n,0} - \hat{g}_n] \quad (98)$$

where we have used (96). Solving for \hat{g}_n yields

$$\hat{g}_n = \left(- \frac{Q}{\Omega_d a^{d-1} c^2} H_{d,n} + \frac{2Q}{c} L^{d/2} \delta_{n,0} \right) \left(\frac{8D\pi^2 n^2 + \frac{2Q}{c}}{L^2} \right)^{-1} \quad (99)$$

This can now be inverted according to (45). The $\mathbf{n} = 0$ term must be separated out explicitly, and the remaining sum can be converted to an integral:

$$g(\mathbf{r}) = 1 - \frac{1}{(2\pi)^{d/2}} \frac{Q}{2\Omega_d a^{d-1} c^2} \int d\mathbf{q} e^{i\mathbf{q}\cdot\mathbf{r}} \frac{H_d(\mathbf{q})}{Dq^2 + (Q/c)} \quad (100)$$

This result agrees with that of Clement et al.,⁵⁹ who, however, used the Smoluchowski boundary condition in their analysis.

Further results again require a separate discussion for each dimension.

A. One Dimension. In one dimension (again with $r = |x|$, where x is the usual Cartesian coordinate) eq 100 becomes

$$g(r) = 1 - \frac{Q}{2\pi DQ^2} \int_0^\infty dq \frac{\cos(qr) \cos(qa)}{q^2 + (Q/DQ)} \\ = 1 - \frac{1}{8} \left(\frac{Q}{DQ^3} \right)^{1/2} (e^{-|r-a|(Q/DQ)^{1/2}} + e^{-|r+a|(Q/DQ)^{1/2}}) \quad (101)$$

This together with relation 96

$$Q = 2kQ^2 g(a) \quad (102)$$

constitutes the solution of the steady-state problem.

The results can be simplified further (and brought to more familiar form) if we take $ka/2D = 1$ [cf. (39)] and if we assume that $aQ \ll 1$, i.e., that there is considerably less than "full occupancy" in the steady state. Setting $r = a$ in (101) and noting that in this case $Qa^2/DQ = 4g(a)aQ \ll 1$, we can expand the exponential. This readily leads to an algebraic equation for $(g(a))^{1/2}$, which in turn can readily be solved to yield

$$g(a) = 4aQ \quad (103)$$

with corrections of higher order in aQ (note that this confirms the consistency of the inequality $Qa^2/DQ \ll 1$). Substitution into (102) then immediately leads to the familiar result⁵⁹

$$Q = 16DQ^3 \quad (104)$$

again with small corrections. Finally, substitution of (104) in (101) then yields for the spatial distribution

$$g(r) = 1 - \frac{1}{2} (e^{-4Q|r-a|} + e^{-4Q|r+a|}) \quad (105)$$

Thus, in the steady state there is again a depletion zone around each reactant particle. The size of this region is inversely proportional to the steady-state density of reactants.

B. Two Dimensions. As in the batch reaction, the two-dimensional expression for the pair correlation function in the steady state

$$g(r) = 1 - \frac{Qa}{DQ^2} I_0(a(D/Q)^{1/2}) K_0(r(D/Q)^{1/2}) \quad (106)$$

does not lend itself to a simple analytic expression for Q as a function of the steady-state density Q nor for the steady-state spatial distribution $g(r)$. In particular, there are again logarithmic deviations from classical behavior that we do not pursue explicitly. It is, however, straightforward to establish that again our results agree with those of Clement et al.⁵⁹

C. Three Dimensions. In three dimensions eq 100 becomes

$$g(r) = 1 - \frac{Q}{4\pi^2 DQ^2 ar} \int_0^\infty dq \frac{\sin(qr) \sin(qa)}{q^2 + (Q/DQ)} \\ = 1 - \frac{1}{16\pi ar} \left(\frac{Q}{DQ^3} \right)^{1/2} (e^{-|r-a|(Q/DQ)^{1/2}} - e^{-|r+a|(Q/DQ)^{1/2}}) \quad (107)$$

This together with relation 96

$$Q = 4\pi a^2 kQ^2 g(a) \quad (108)$$

again constitutes the solution of the steady-state problem.

The results can again be simplified if we set $ka/2D = 1$ and if in the steady state there is much less than full occupancy, i.e., $a^3Q \ll 1$. Setting $r = a$ in (107) and expanding the exponential (which is again justified with these assumptions), we obtain

$$g(a) = 1/2 \quad (109)$$

with corrections of higher order in $aQ^{1/3}$. This result in (108) in turn leads to

$$Q = 4\pi a DQ^2 \quad (110)$$

The spatial distribution of reactants in the steady state obtained from (107) with (110) then finally is

$$g(r) = 1 - \frac{a}{2r} e^{-(r-a)(4\pi aQ)^{1/2}} \quad (111)$$

Thus, in three dimensions there is no depletion zone in the steady state—the distribution is essentially uniform.⁵⁹

V. Simulations

We have carried out a number of numerical simulations of the $A + A \rightarrow 0$ reaction in order to test some of the results predicted by our theory. In this section we present the results of these simulations and the comparison with our predictions.

A. Methods. The numerical simulations of the chemical reaction are performed using the conventional techniques described in our earlier papers.^{73,89-91} Briefly, lattices of 10^6 sites in one dimension and square lattices of size 2000×2000 in two dimensions are generated. Particles are initially placed at random on the lattice with the restriction that only one particle can occupy a given site at any time. We impose cyclic boundary conditions on the lattices. The reaction then proceeds in the usual way: the particles diffuse on the lattice by performing independent forced random walks to nearest neighbor sites. When two particles step onto the same site, they react, which means that they are removed from the system. Cyclic boundary conditions are applied at the ends of the lattice to the random walk as well. We monitor the particle density as a function of time for times up to 10^4 steps, and this immediately yields the global rate of the reaction. We also monitor in one dimension the number of A-A pairs (that is, the number of pairs of particles on adjacent sites) and the number of A-0-A pairs (that is, the number of pairs of particles separated by exactly one empty site). For two dimensions we also monitor the A-A and A-0-A pairs, but in addition we also monitor the bent A-0-A pairs which we denote by $bA-0-A$, by which we mean the case where the two A-0 bonds form a 90° angle (as opposed to the straight line A-0-A configuration).

Correlation functions in one dimension are calculated as follows. For each particle, at a fixed time t after the beginning of the simulation, we count n , the number of all other particles present in a sampling interval Δ at a distance l away from the particle (point of origin). Typically $\Delta = 10$ sites, and we go up to $l = 1000$ sites in both directions from the point of origin. We average the results over all particles. The properly normalized correlation function is then given by

$$g(l,t) = \frac{n}{2Nl} \Delta \quad (112)$$

where N is the total number of particles present in the system at time t . Thus $g(l,t)$ gives the normalized probability of finding at time t a particle within a distance Δ at a distance l away from a particle known to be at the origin.

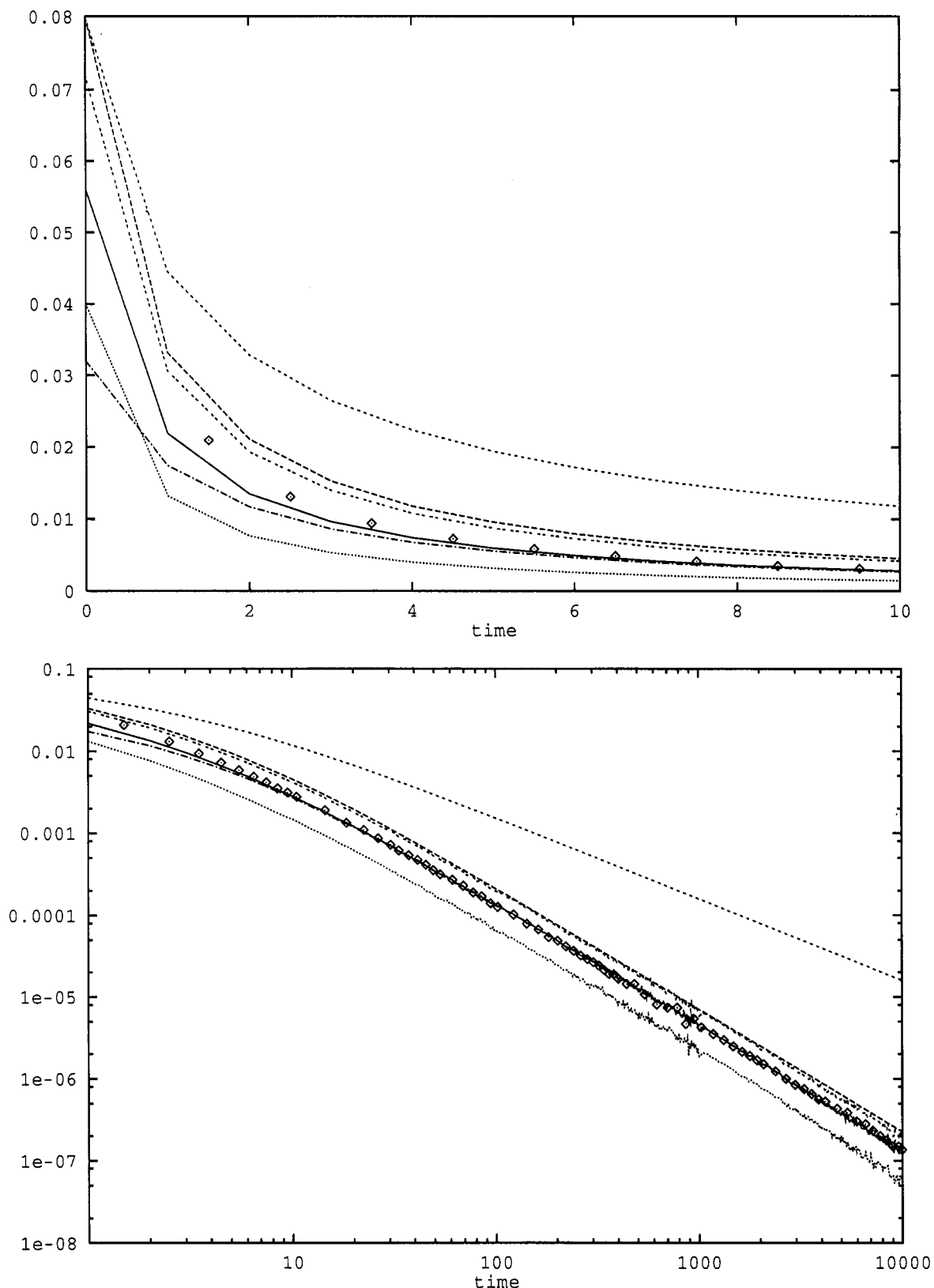


Figure 1. Simulation results for the reaction rate vs time for one-dimensional lattices (diamonds). Simulations are carried out on lattices of 10^6 sites with initial density $\rho_0 = 0.2$, and results are averaged over 100 runs. The curves involve the density ρ of A particles, the density ρ_{AA} of nearest neighbor pairs, and the density ρ_{A0A} of pairs separated by exactly one empty site. The following combinations (from top to bottom at $t = 4$) are shown as a function of time: (i) $2\rho^2(t)$, (ii) $10\rho^3(t)$, (iii) $\rho_{AA} + \rho_{A0A}$, (iv) $\rho_{AA} + \frac{1}{2}\rho_{A0A}$, (v) ρ_{A0A} , and (vi) ρ_{AA} . The short-time behavior is shown in a on a linear scale; the long-time behavior is shown in b on a log-log scale.

The results of this section are presented in terms of discrete lattice simulations; our analytic results are of course based on the continuum reaction-diffusion model. Although we often use the same symbols in both cases, the context makes the usage clear.

B. Results. Figures 1 and 2 deal with the reaction rate as a function of time for batch reactions in one and two dimensions, respectively. Part a of each figure plots various quantities described below as a function of time on linear scales, and its purpose is to show the short-time behavior of the various

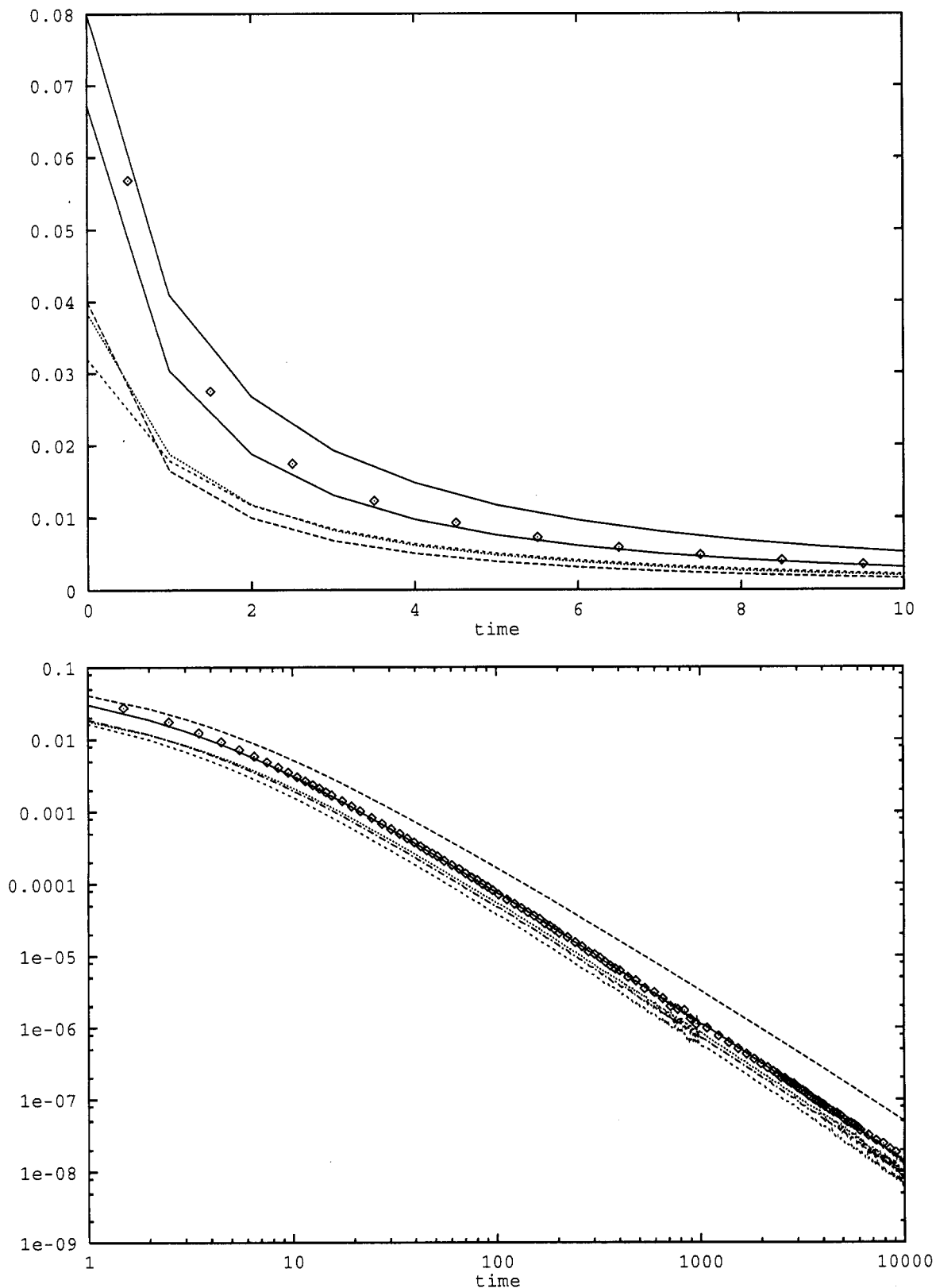


Figure 2. Simulation results for the reaction rate vs time for two-dimensional lattices (diamonds). Simulations are carried out on lattices of 4×10^6 sites with initial density $\rho_0 = 0.2$, and the results are averaged over 1000 runs. Here, in addition to the densities defined for the one-dimensional case, we distinguish between the density ρ_{A0A} of pairs of particles in a linear configuration separated by exactly one empty site, and the density ρ_{bA0A} of pairs where the two A-O bonds form a 90° angle. The curves (from top to bottom at $t = 4$) represent the following combinations as a function of time: (i) $2\rho^2(t)$; (ii) $\frac{1}{2}\rho_{AA} + \frac{1}{4}\rho_{bA0A} + \frac{1}{8}\rho_{A0A}$; (iii) $\frac{1}{2}\rho_{AA}$; (iv) $\frac{1}{2}\rho_{bA0A}$; and (v) $\frac{1}{2}\rho_{A0}$. The short-time behavior is shown in a on a linear scale and the long-time behavior in b on a log-log scale.

quantities, while part b shows the same quantities as a function of time on a log-log scale that allows the discussion of the long-time behavior of these quantities.

We begin with our one-dimensional results, obtained for lattices of 10^6 sites with an initial density of $\rho_0 = 0.2$ (that is,

one out of every five sites is initially occupied), and results are averaged over 1000 runs. The diamonds are the number of particles reacting per unit volume per unit time, i.e., the reaction rate obtained from our simulations. The curves are ordered in our description below from top to bottom in the order in which

they occur in Figure 1a at $t = 4$. The curves essentially retain this ordering or become indistinguishable at all times beyond $t = 4$. The top curve is $2\rho^2(t)$, and the second curve is $10\rho^3(t)$. The coefficients (2 and 10) are not significant and are chosen purely for convenience to visually separate the various curves from one another. Thus, the upper curve is proportional to the reaction rate in a classical bimolecular reaction and should describe the behavior of our system at very short times; the second curve is proportional to the asymptotic form (76) and should describe the reaction rate at very long times. Indeed, the diamonds are parallel to the upper curve at very early times and to the lower curve at later times. In Figure 1b the strong deviation of the reaction rate (diamonds) from the ρ^2 curve (upper curve) is clearly apparent, as is the fact that the ρ^3 curve (second from top) runs parallel to the reaction rate results. These results are thus consistent with the nonclassical asymptotic rate law (76).

The remaining curves attempt to establish the consistency of our assumption that the rate of the reaction is directly proportional to the two-particle correlation function, as in (20). In our discrete lattice formulation, this corresponds to the assumption that the rate of the reaction depends on the density of nearest neighbor pairs (denoted by ρ_{AA}) and next nearest neighbor pairs (denoted by ρ_{A0A}). In our simulations the probability per unit time that a nearest neighbor pair annihilates is twice the probability per unit time that a next nearest neighbor pair does so (as can be clearly seen by considering the jumping options in the two configurations). Therefore, our model assumes that the reaction rate is equal to $\rho_{AA} + \frac{1}{2}\rho_{A0A}$. In both parts of Figure 1 the fourth curve from the top is this latter combination, and it is clear that it coincides with the reaction rate diamonds. The third curve from the top is the combination $\rho_{AA} + \rho_{A0A}$, the fifth and sixth are respectively ρ_{A0A} and ρ_{AA} , and all of these are essentially parallel to the reaction rate. This would appear to indicate that there is a specific proportionality relation between ρ_{AA} and ρ_{A0A} . We have not established such a relation on theoretical grounds. Note that this proportionality can be translated in the continuum approach to a proportionality between the pair correlation function of adjacent particles and of slightly more distant particles (contributions to the correlations between slightly more distant particles from groups of three particles that are close together, such as might be represented by ρ_{AAA} in the discrete model, are small for low densities). Note that the initial values $\rho_{AA}(0)$ and $\rho_{A0A}(0)$ for the nearest neighbor and next nearest neighbor pair densities are those for a random distribution of reactants and can be calculated exactly.⁹² The values obtained from our simulations shown in Figure 1a agree exactly with the calculated values.

Consider now our two-dimensional simulation results shown in Figure 2. The results are obtained for lattices of 4×10^6 sites, again with an initial density $\rho_0 = 0.2$, and results are again averaged over 1000 runs. The curves in our description are ordered as they occur from top to bottom at $t = 4$ in Figure 2a. The top curve is $2\rho^2(t)$, and the rate of the reaction as represented by the diamonds runs essentially parallel to this curve. Recall that in two dimensions the deviations from classical behavior are only logarithmic, as noted in section IIIB.

The second curve from the top is the combination $\frac{1}{2}\rho_{AA} + \frac{1}{4}\rho_{bA0A} + \frac{1}{8}\rho_{A0A}$. If our model relating the reaction rate to the pair correlation function is correct, the rate of the reaction (diamonds) should coincide with this curve. Indeed this is the case, as clearly seen in both parts of Figure 2. The remaining three curves are ρ_{AA} (density of nearest neighbor pairs), ρ_{bA0A} (density of bent next nearest neighbor pairs), and ρ_{A0A} (density of linear next nearest neighbor pairs). Again, these results would

indicate a specific proportionality between these three quantities that we have not pursued theoretically.

We stress a point that is made particularly evident by this presentation: the reaction rate is determined entirely by the particle arrangements in the small shell of *nearest and next nearest neighbors* on the lattices. Anomalous kinetics is a direct reflection of the deviations of these near neighbor two-particle distributions from their values for a random distribution of particles. Dependence on other quantities is of course implicit insofar as the determination of the distribution of nearest and next nearest neighbor pairs is a many-body problem.

In Figure 3 we show the correlation function $g(r,t)$ obtained from our one-dimensional simulations. In Figure 3a the correlation function is shown as a function of distance r (in appropriate discrete units) for various fixed times: from top to bottom the times are $t = 10^2, 10^3, 10^4, 10^5, 10^6$. The increasing noisiness of the curves with increasing time reflects the presence of fewer particles and the resultant deterioration in the statistics. As expected, at each time the correlation function approaches unity at long distances, and also, as predicted, the depletion zone develops and grows around $r = 0$ with increasing time. In order to test the scaling implicit in eq 79, we have replotted all these curves in Figure 3b as a function of the scaled distance $r/2(Dt)^{1/2}$ with $D = \frac{1}{2}$. The scaling is seen to be excellent. There is, however, a difference of a factor $2^{1/2}$ between this scaled distance and the argument of eq 79. This difference is certainly a consequence of our truncation approximation. The fact that the error simply appears as a numerical factor, i.e., as an effective renormalization of the parameters, indicates that higher order correlation functions that have been ignored or approximated are indeed simply related to the lower order ones. This is consistent with the proportionality between nearest and next nearest neighbor pair densities noted earlier.

VI. Smoluchowski Boundary Condition

We noted earlier that a Smoluchowski-type approach to the problem considered here would describe the process by the hierarchy of eqs 37–41 in place of eqs 32 and 31. It is useful to compare the results for the two cases.

Consider first the batch reactions. Differences in the two approaches first appear in a substantial way in (57), which is now replaced by

$$\tilde{g}(\mathbf{r},s) = \tilde{g}_0(\mathbf{r},s) - 2D\tilde{g}'(a,s)\tilde{K}_d(\mathbf{r},s) \quad (113)$$

where the prime denotes a spatial derivative. To find g' on the right hand side we again set $r = a$. Since the Smoluchowski boundary condition (41) imposes a zero value on $g(a,t)$, eq 65 is now replaced by

$$0 = \tilde{g}_0(a,s) - 2D\tilde{g}'(a,s)\tilde{K}_d(a,s) \quad (114)$$

This expression is then solved for $\tilde{g}'(a,s)$ and the solution inserted in (57) to obtain in place of (68)

$$\tilde{g}(r,s) = \tilde{g}_0(r,s) - \frac{\tilde{g}_0(a,s)\tilde{K}_d(r,s)}{\tilde{K}_d(a,s)} \quad (115)$$

Note that in obtaining this result the boundary condition $g(a,t) = 0$ had to be explicitly imposed (i.e., it is not a "natural" boundary condition) and was essential in obtaining this result. Were one not to use this condition but instead proceed (in the spirit of our approach) by taking a spatial derivative of (113), setting $r = a$, and solving for g' , one would find a reaction term that would for all time depend on the initial condition, which is of course known to be incorrect.

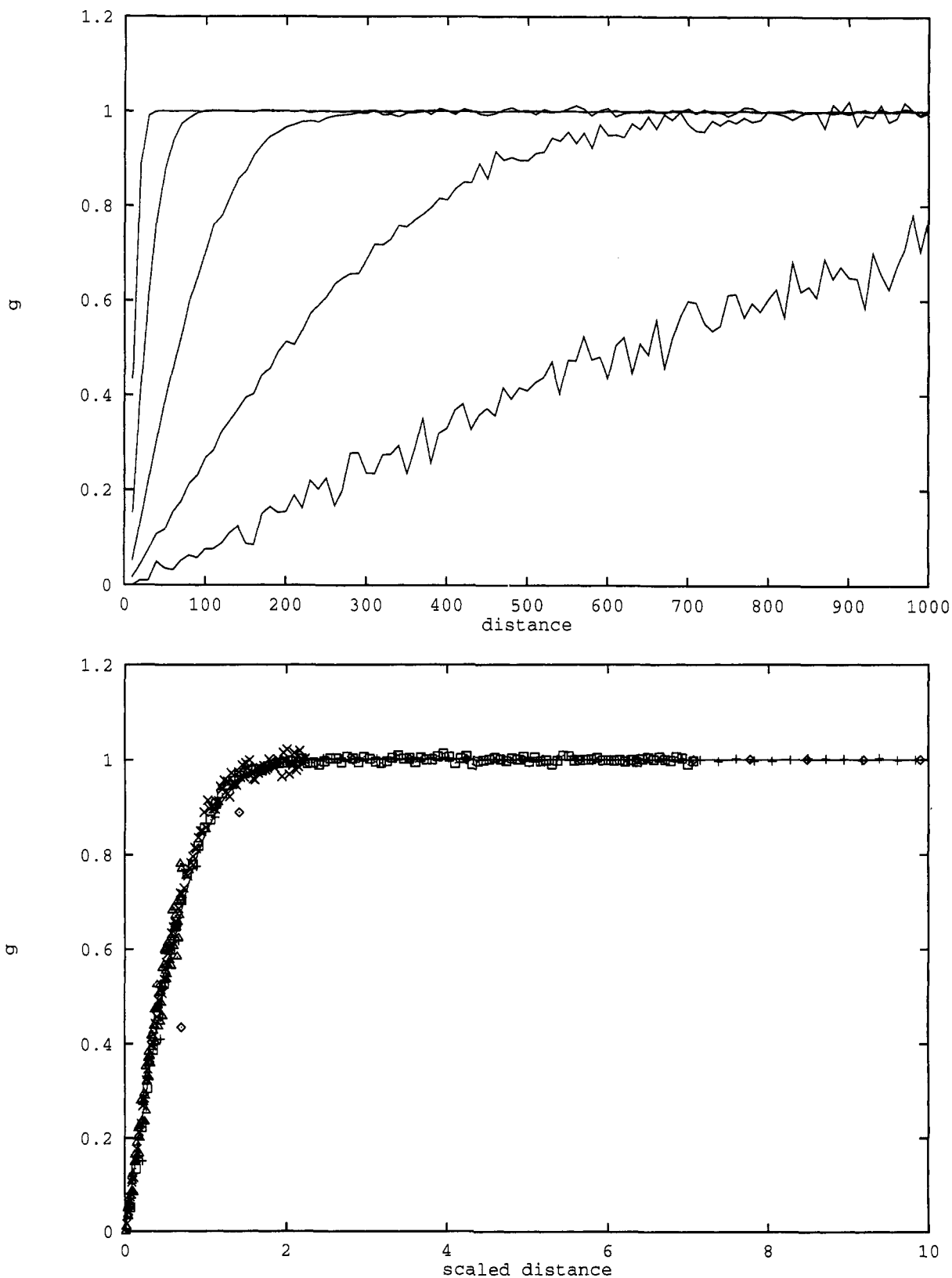


Figure 3. Correlation function in one dimension vs distance. (a) Correlation function vs unscalled distance r for various times; times from left to right are 10^2 , 10^4 , 10^5 , and 10^6 . (b) Correlation function vs scaled distance $r/(2t)^{1/2}$. Symbols: diamonds ($t = 10^2$), pluses ($t = 10^3$), squares ($t = 10^4$), crosses ($t = 10^5$), and triangles ($t = 10^6$). The continuous curve is $\text{erf}[r/(2t)^{1/2}]$.

What are the differences in the explicit results for the rate law and correlation functions for batch reactions? In one dimension (115) leads to exactly the same results as we have obtained, that is, to precisely the same rate law (76) and the same correlation function (79). Because analytic expressions are difficult to obtain in two dimensions, we have not carried through the corresponding analysis. In three dimensions we

find

$$\tilde{g}'(a,s) \sim 1/as \quad (116)$$

and therefore

$$g'(a,t) \sim 1/a \quad (117)$$

Consequently we find the rate law

$$\dot{Q} = -8\pi DaQ^2 \quad (118)$$

The rate coefficient here is twice that of our model, (91), but the results are otherwise the same. In either case the rate law has the classical form. For the spatial distribution of reactants we now find in place of (92)

$$\begin{aligned} \tilde{g}(r,s) &\sim \frac{1}{s} \left(1 - \frac{\tilde{K}_3(r,s)}{\tilde{K}_3(a,s) + a/2D} \right) \\ &\sim \frac{1}{s} \left[1 - \left(\frac{a}{2r(2Ds)^{1/2}} (e^{-(s/2D)^{1/2}|r-a|} - e^{-(s/2D)^{1/2}|r+a|}) \right) \right. \\ &\quad \left. - \frac{1}{2(2Ds)^{1/2}} (1 - e^{-2(s/2D)^{1/2}a}) \right] \quad (119) \end{aligned}$$

For $(s/2D)^{1/2}a \ll 1$ and $a \leq r$ this reduces to

$$\tilde{g}(r,s) \sim \frac{1}{s} \left[1 - \frac{a}{r} e^{-(s/2D)^{1/2}(r-a)} \right] \quad (120)$$

and inverse Laplace transformation of this expression immediately yields

$$g(r,t) \sim 1 - \frac{a}{r} \operatorname{erfc} \left(\frac{r-a}{2(2Dt)^{1/2}} \right) \quad (121)$$

in place of (95). The spatial distribution thus again differs from ours simply by a numerical factor and again approaches a uniform one (except for corrections of order a). Note that (121) obeys the Smoluchowski boundary condition $g(a,t) = 0$, while with (95) $g(a,t) \sim O(a)$.

Let us next turn to a comparison of the steady-state results. In one dimension we first set $g(a) = 0$ (Smoluchowski boundary condition) in eq 101,

$$g(a) = 0 = 1 - \frac{1}{8} \left(\frac{Q}{DQ^3} \right)^{1/2} (1 + e^{-2a(Q/DQ)^{1/2}}) \quad (122)$$

i.e.,

$$Q = 16DQ^3 + O(aQ) \quad (123)$$

in agreement with (104) to leading order in a . Note that truncation of (123) at the first term is associated with a $g(a)$ that is not exactly zero but that vanishes only to first order in a —exactly as in our approach. In other words, $g(a)$ is exactly zero only if the corrections to Q of all orders in a are included. Finally, if we retain only the leading term in (123) (so that $g(a)$ is not exactly zero), then substitution back into (101) leads exactly to (105) for the spatial distribution of reactants. The steady-state results in two and three dimensions are also the same as those found earlier to within physically unimportant corrections.

The essential equivalence of the results obtained with our approach to the diffusion-limited reaction and the Smoluchowski-type formulation is of course not surprising (see the discussion in the Introduction). This essential equivalence is also embodied in our simulation results through the proportionality that is observed between the nearest and next nearest neighbor densities Q_{AA} and Q_{A0A} . In the last section we related the pair correlation function in our theory to a particular combination of these two quantities. Clearly, the gradient of the pair correlation function which appears in the Smoluchowski-type approach can be related to an appropriate difference between these quantities. Since they are observed to be

proportional to one another in the parameter regimes studied here, the reaction terms in the two approaches are proportional to each other and there is at most a numerical difference (as observed) in the prefactor in the resultant reaction rate laws. As mentioned earlier and as can clearly be seen from our formulas, differences would occur if one departs from the diffusion-limited regime and allows the rate coefficient k to be small relative to D/a .

VII. Summary and Conclusions

In this section we summarize the salient points of our analysis. We have formulated an approach to the $A + A \rightarrow$ products reaction that is based on a reaction-diffusion equation frequently used for the $A + B$ problem but requires appropriate generalization for the $A + A$ problem. Starting from this reaction-diffusion equation, we have constructed the first equations in a moment hierarchy whose first two members are the global density of A particles and the pair correlation function. We terminate the hierarchy via an approximation that relates the three-particle correlation function to two-particle correlation functions and thereby obtain a set of coupled equations that turns out to be linear and hence analytically tractable.

This approach leads naturally to the proportionality of the rate of the reaction to the pair correlation function evaluated at $r = a$, where a is the diameter of the reacting particles. In other words, the reaction rate is proportional to the probability that two A particles are sufficiently close. In the more traditional approach based on the Smoluchowski theory for trapping phenomena, the reaction rate is instead proportional to the gradient of the pair correlation function. We have noted the differences and essential similarities between these points of view and their consequences.

We have presented numerical simulations in one and two dimensions in order to check our predictions. We confirm the well-known anomalous rate law in one dimension (the anomalies are marginal in two dimensions), and the proportionality of the reaction rate to the two-particle correlation function. Our simulations serve to stress an important point also brought forth by the theory: the rate of the reaction is determined entirely by the spatial distribution of a very small shell of particles around a given reactant particle. In the lattice simulations, the rate is entirely determined by the distribution of nearest and next nearest pairs. In the continuum formulation this translates into the distribution of reactants that are very close (in physical contact) with a given reactant particle. Anomalous kinetics is a direct reflection of the deviation of the spatial distribution of this small shell from a random configuration.

We have also presented simulation results that confirm the predicted distance and time scaling of the pair correlation function in one dimension.

It must be stressed that the conclusions arrived at in this work, in particular the observation that the reaction rate is determined by the configuration of particles immediately surrounding a given reactant particle and the consequences of this locality, are in turn obtained only because we have restricted our analysis to local interparticle interactions. The situation would be completely different if two particles could react at longer range, for example, if the reaction rate between pairs of particles would depend on the distance between them as a power law.

Acknowledgment. We gratefully acknowledge support from the Department of Energy Grant DE-FG03-86ER13606 (K.L.), from the National Science Foundation Grant DMR-91-11622 (R.K.), and from NATO Grant CRG 920029 (P.A.).

References and Notes

- (1) Bramson, M.; Griffeath, D. Z. *Wahrscheinlichkeitstheorie Gebiete* 1980, 53, 183.

- (2) Bramson, M.; Griffeath, D. Z. *Ann. Probab.* **1980**, *8*, 183.
- (3) Klymko, P. W.; Kopelman, R. *J. Lumin.* **1981**, *24/25*, 457.
- (4) Klymko, P. W.; Kopelman, R. *J. Phys. Chem.* **1982**, *86*, 3686.
- (5) Klymko, P. W.; Kopelman, R. *J. Phys. Chem.* **1983**, *87*, 4565.
- (6) Torney, D. C.; McConnell, H. M. *J. Phys. Chem.* **1983**, *87*, 1441.
- (7) Torney, D. C. *J. Chem. Phys.* **1983**, *79*, 3606.
- (8) Torney, D. C.; McConnell, H. M. *Proc. R. Soc. London A* **1983**, *387*, 147.
- (9) Keizer, J. J. *J. Chem. Phys.* **1983**, *79*, 4877.
- (10) Kopelman, R.; Hoshen, J.; Newhouse, J. S.; Argyrakis, P. *J. Stat. Phys.* **1983**, *30*, 335.
- (11) Blumen, A.; Klafter, J.; Zumofen, G. *Phys. Rev. B* **1983**, *27*, 3429.
- (12) de Gennes, P. G. *Chem. R. Acad. Sci. Paris* **1983**, *296*, 881.
- (13) Evesque, P. *J. Phys.* **1983**, *44*, 1217.
- (14) Evesque, P.; Duran, J. *J. Chem. Phys.* **1984**, *80*, 3016.
- (15) Kang, K.; Redner, S. *Phys. Rev. Lett.* **1984**, *52*, 955.
- (16) Elyutin, P. V. *J. Phys. C* **1984**, *17*, 1867.
- (17) Kopelman, R.; Klymko, P. W.; Newhouse, J. S.; Anacker, L. *Phys. Rev. B* **1984**, *29*, 3747.
- (18) Meakin, P.; Stanley, H. E. *J. Phys. A* **1984**, *173*, L17.
- (19) Anacker, L. W.; Kopelman, R.; Newhouse, J. S. *J. Stat. Phys.* **1984**, *36*, 591.
- (20) Newhouse, J. S.; Argyrakis, P.; Kopelman, R. *Chem. Phys. Lett.* **1984**, *107*, 48.
- (21) Kang, K.; Meakin, P.; Oh, J. H.; Redner, S. *J. Phys. A* **1984**, *17*, L665.
- (22) Anacker, L. W.; Kopelman, R. *J. Chem. Phys.* **1984**, *81*, 6402.
- (23) Anacker, L. W.; Parson, R. P.; Kopelman, R. *J. Phys. Chem.* **1985**, *89*, 4785.
- (24) Racz, Z. *Phys. Rev. Lett.* **1985**, *55*, 1707.
- (25) Kang, K.; Redner, S. *Phys. Rev. A* **1985**, *32*, 435.
- (26) Elskens, Y.; Frish, H. L. *Phys. Rev. A* **1985**, *31*, 3812.
- (27) Newhouse, J. S.; Kopelman, R. *Phys. Rev. B* **1985**, *31*, 1677.
- (28) Kopelman, R. *J. Phys. C* **1985**, *7*, 9.
- (29) Zumofen, G.; Blumen, A.; Klafter, J. *J. Chem. Phys.* **1985**, *82*, 3198.
- (30) Ben-Avraham, D.; Redner, S. *Phys. Rev. A* **1986**, *34*, 501.
- (31) Newhouse, J. S.; Kopelman, R. *J. Chem. Phys.* **1986**, *85*, 6804.
- (32) Kopelman, R.; Parus, S.; Prasad, J. *Phys. Rev. Lett.* **1986**, *56*, 1742.
- (33) Kopelman, R. *J. Stat. Phys.* **1986**, *42*, 185.
- (34) Peliti, L. *J. Phys. A* **1986**, *19*, L365.
- (35) Ben-Avraham, D. *J. Stat. Phys.* **1987**, *48*, 315.
- (36) Lushnikov, A. A. *Phys. Lett. A* **1987**, *120*, 135.
- (37) Redner, S.; Ben-Avraham, D.; Kahng, B. *J. Phys. A* **1987**, *20*, 1231.
- (38) Kopelman, R. *Philos. Mag. B* **1987**, *56*, 717.
- (39) Prasad, J.; Kopelman, R. *J. Phys. Chem.* **1987**, *91*, 265.
- (40) Prasad, J.; Kopelman, R. *Phys. Rev. Lett.* **1987**, *59*, 2103.
- (41) Argyrakis, P.; Kopelman, R. *J. Phys. Chem.* **1987**, *91*, 2699.
- (42) Li, L.; Kopelman, R. *J. Lumin.* **1988**, *40/41*, 688.
- (43) Peacock-López, E.; Keizer, J. J. *J. Chem. Phys.* **1988**, *88*, 1997.
- (44) Balding, D.; Clifford, P.; Green, N. J. B. *Phys. Lett. A* **1988**, *126*, 481.
- (45) Kanno, S. *Prog. Theoret. Phys.* **1988**, *79*, 1330.
- (46) Spouge, J. L. *Phys. Rev. Lett.* **1988**, *60*, 871, 1885.
- (47) Kuzovkov, V.; Kotomin, E. *Rep. Prog. Phys.* **1988**, *51*, 1479.
- (48) Doering, C. R.; Ben-Avraham, D. *Phys. Rev. A* **1988**, *38*, 3035.
- (49) Blumen, A.; Zumofen, G.; Klafter, J. In *Fractals, Quasicrystals, Chaos, Knots and Algebraic Quantum Mechanics*; Amann, A., et al., Eds.; Kluwer: New York, 1989; p 21.
- (50) Kopelman, R. *Science* **1988**, *41*, 1620.
- (51) Kopelman, R.; Parus, S. J.; Prasad, J. *Excited State Relaxation and Transport Phenomena in Solids*. Skinner, J. L., Fayer, M. D., Eds. *Chem. Phys.* **1988**, *128*, 209 (special issue).
- (52) Cheng, Z.; Redner, S.; Leyvraz, F. *Phys. Rev. Lett.* **1989**, *62*, 2321.
- (53) Doering, C. R.; Ben-Avraham, D. *Phys. Rev. Lett.* **1989**, *62*, 2563.
- (54) Kopelman, R.; Parus, S. J.; Shi, Z.-Y. In *Dynamical Processes in Condensed Molecular Systems*; Klafter, J., Jortner, J., Blumen, A., Eds.; World Scientific: Singapore, 1989; p 231.
- (55) Parus, S. J.; Kopelman, R. *Phys. Rev. B* **1989**, *39*, 889.
- (56) Argyrakis, P.; Kopelman, R. *J. Phys. Chem.* **1989**, *93*, 225.
- (57) Parus, S. J.; Kopelman, R. *Mol. Cryst. Liq. Cryst.* **1989**, *175*, 119.
- (58) Burlatskii, S. F.; Ovchinnikov, A. A.; Oshanin, G. S. *Sov. Phys. JETP* **1989**, *68*, 1153.
- (59) Clement, E.; Sander, L. M.; Kopelman, R. *Phys. Rev. A* **1989**, *39*, 6472.
- (60) Prasad, J.; Kopelman, R. *Chem. Phys. Lett.* **1989**, *157*, 535.
- (61) Harmon, L. A.; Kopelman, R. *J. Phys. Chem.* **1990**, *94*, 3454.
- (62) Argyrakis, P.; Kopelman, R. *Phys. Rev. A* **1990**, *41*, 2114.
- (63) Prasad, J.; Kopelman, R. *J. Lumin.* **1990**, *45*, 258.
- (64) Kopelman, R.; Li, C. S.; Shi, Z.-Y. *J. Lumin.* **1990**, *45*, 40.
- (65) Kopelman, R.; Anacker, L. W.; Clement, E.; Li, L.; Sander, L. J. *Lumin.* **1990**, *45*, 323.
- (66) Parus, S. J.; Kopelman, R. *J. Lumin.* **1990**, *45*, 43.
- (67) Shi, Z.-Y.; Kopelman, R. *J. Lumin.* **1990**, *45*, 275.
- (68) Kopelman, R. In *Dynamical Processes in Condensed Molecular Systems*; Blumen, A., Klafter, J., Haarer, D., Eds.; World Scientific: Singapore, 1990; p 173.
- (69) Ohtsuki, T. *Phys. Rev. A* **1991**, *43*, 6917.
- (70) Privman, V. *J. Stat. Phys.* **1992**, *69*, 629.
- (71) Li, L.; Kopelman, R. *J. Phys. Chem.* **1992**, *96*, 8079.
- (72) Shi, Z.-Y.; Kopelman, R. *Chem. Phys.* **1992**, *167*, 149.
- (73) Argyrakis, P.; Kopelman, R. *Phys. Rev. A* **1992**, *45*, 5814.
- (74) Shi, Z.-Y.; Kopelman, R. In *Dynamics in Small Confining Systems*; Drake, J. M., Klafter, J., Kopelman, R., Awshalom, D. D., Eds.; MRS Symposium Proceedings; Materials Research Society: New York, 1993; Vol. 290, p 279.
- (75) Kopelman, R.; Shi, Z.-Y.; Li, C.-S. *J. Lumin.* **1991**, *48/49*, 143, and references cited therein.
- (76) Noyes, R. M. In *Progress in Reaction Kinetics*, Vol. 1; Porter, G., Ed.; Pergamon: London, 1961.
- (77) Lindenberg, K.; West, B. J.; Kopelman, R. In *Noise and Chaos in Nonlinear Dynamical Systems*; Capelin, S., Moss, F., Eds.; Cambridge University Press: Cambridge, U.K., 1989; and references cited therein.
- (78) Lindenberg, K.; West, B. J.; Kopelman, R. *Phys. Rev. A* **1990**, *42*, 890.
- (79) Lindenberg, K.; West, B. J.; Kopelman, R. *Phys. Rev. Lett.* **1988**, *60*, 1777.
- (80) Collins, F. C.; Kimball, G. E. *J. Colloid Sci.* **1949**, *4*, 425.
- (81) von Smoluchowski, M. *Z. Phys. Chem.* **1917**, *92*, 129.
- (82) Sveshnikoff, B. *Acta Physicochim. URSS* **1935**, *3*, 257.
- (83) Waite, T. R. *Phys. Rev.* **1957**, *107*, 463, 471.
- (84) Monchik, L.; Magee, J. K.; Samuel, A. H. *J. Chem. Phys.* **1957**, *26*, 935.
- (85) Wilemski, G.; Fixman, M. *J. Chem. Phys.* **1973**, *58*, 4009; **1976**, *64*, 4559.
- (86) van Kampen, N. G. *Int. J. Quantum Chem.* **1982**, *16*, 101.
- (87) de Gennes, P. G. *J. Phys. Chem.* **1982**, *76*, 3316.
- (88) Keizer, J. J. *J. Phys. Chem.* **1982**, *86*, 5052.
- (89) Argyrakis, P.; Kopelman, R. *Phys. Rev. A* **1990**, *41*, 2114, 2121.
- (90) Argyrakis, P. *Comput. Phys.* **1992**, *6*, 525.
- (91) Blumen, A.; Luding, S.; Sokolov, I. M. *J. Stat. Phys.* **1991**, *65*, 849.
- (92) Hoshen, J.; Kopelman, R. *Phys. Stat. Sol.* **1977**, *81*, 479.